AFRL-RZ-WP-TP-2008-2111

TOWARD THE EXPANSION OF LOW-PRESSURE-TURBINE AIRFOIL DESIGN SPACE (POSTPRINT)

T. J. Praisner, E.A. Grover, D.C. Knezevici, I. Popovic, S.A. Sjolander, J.P. Clark, R. Sondergaard, and P.J. Koch

Turbine Branch
Turbine Engine Division

APRIL 2008

AIR FORCE RESEARCH LABORATORY
PROPULSION DIRECTORATE
WRIGHT-PATTERSON AIR FORCE BASE, OH 45433-7251
AIR FORCE MATERIEL COMMAND
UNITED STATES AIR FORCE

REPORT DOCUMENTATION PAGE

Form Approved
OMB No. 0704-0188

1. REPORT DATE *(DD-MM-YY)*	2. REPORT TYPE	3. DATES COVERED *(From - To)*
April 2008	Conference Paper Postprint	01 October 2007 – 19 December 2007

4. TITLE AND SUBTITLE
TOWARD THE EXPANSION OF LOW-PRESSURE-TURBINE AIRFOIL DESIGN SPACE (POSTPRINT)

5a. CONTRACT NUMBER
In-house

5b. GRANT NUMBER

5c. PROGRAM ELEMENT NUMBER
62203F

6. AUTHOR(S)
T. J. Praisner and E.A. Grover (United Technologies, Pratt & Whitney)
D.C. Knezevici, I. Popovic, and S.A. Sjolander (Carleton University)
J.P. Clark, R. Sondergaard, and P.J. Koch (AFRL/RZTT)

5d. PROJECT NUMBER
3066

5e. TASK NUMBER
06

5f. WORK UNIT NUMBER
306606W8

7. PERFORMING ORGANIZATION NAME(S) AND ADDRESS(ES)
United Technologies, Pratt & Whitney
East Hartford, CT

Carleton University
Department of Mechanical and Aerospace Engineering
Ottawa, ON, Canada

Turbine Branch (AFRL/RZTT)
Turbine Engine Division
Air Force Research Laboratory, Propulsion Directorate
Wright-Patterson Air Force Base, OH 45433-7251
Air Force Materiel Command, United States Air Force

8. PERFORMING ORGANIZATION REPORT NUMBER
AFRL-RZ-WP-TP-2008-2111

9. SPONSORING/MONITORING AGENCY NAME(S) AND ADDRESS(ES)
Air Force Research Laboratory
Propulsion Directorate
Wright-Patterson Air Force Base, OH 45433-7251
Air Force Materiel Command
United States Air Force

AFOSR/NA
875 North Randolph Street
Suite 325, Room 3112
Arlington, VA 22203-1768

10. SPONSORING/MONITORING AGENCY ACRONYM(S)
AFRL/RZTT

11. SPONSORING/MONITORING AGENCY REPORT NUMBER(S)
AFRL-RZ-WP-TP-2008-2111

12. DISTRIBUTION/AVAILABILITY STATEMENT
Approved for public release; distribution unlimited.

13. SUPPLEMENTARY NOTES
Conference paper published in the Proceedings of the GT2008 ASME TURBO EXPO 2008: Power for Land, Sea, and Air, June 9 - 13, 2008, Berlin, Germany.

 Technical paper contains color. PAO Case Number: WPAFB 07-0748, 19 Dec 2007.

14. ABSTRACT
Future engine requirements, including high-altitude flight of unmanned air vehicles as well as a movement to reduce engine cost and weight, are challenging the current state of the art in low-pressure-turbine airfoil design. These new requirements present low-Reynolds number challenges as well as the need for high-performance high-lift design concepts. Here we report on an effort to expand the relatively well established design space for low-pressure turbine airfoils. Analytical and experimental mid-span performance data and loadings are presented for four new airfoil designs based on the Pack B velocity triangles. The new designs represent a systematic expansion of low-pressure turbine airfoil design space through the application of high-lift design concepts for front- and aft-loaded airfoils. Taken holistically, the results presented here demonstrate accurate transition modeling provides a reliable method to develop optimized, very high-lift airfoil designs.

15. SUBJECT TERMS
Turbomachinery, low pressure turbines, transition, turbine design

16. SECURITY CLASSIFICATION OF:			17. LIMITATION OF ABSTRACT:	18. NUMBER OF PAGES	19a. NAME OF RESPONSIBLE PERSON (Monitor)
a. REPORT	b. ABSTRACT	c. THIS PAGE			John P. Clark
Unclassified	Unclassified	Unclassified	SAR	14	19b. TELEPHONE NUMBER *(Include Area Code)* N/A

Standard Form 298 (Rev. 8-98)
Prescribed by ANSI Std. Z39-18

Proceedings of GT2008
ASME TURBO EXPO 2008: Power for Land, Sea, and Air
June 9-13, 2008, Berlin, Germany

GT2008-50898

TOWARD THE EXPANSION OF LOW-PRESSURE-TURBINE AIRFOIL DESIGN SPACE

T. J. Praisner and E. A. Grover
United Technologies, Pratt & Whitney
East Hartford, CT, USA

D. C. Knezevici, I. Popovic, and S. A. Sjolander
Department of Mechanical and Aerospace Engineering
Carleton University, Ottawa, ON, CANADA

J. P. Clark, R. Sondergaard, and P. J. Koch
Air Force Research Laboratory
WP, OH, USA

ABSTRACT

Future engine requirements, including high-altitude flight of unmanned air vehicles as well as a movement to reduce engine cost and weight, are challenging the current state of the art in low-pressure-turbine airfoil design. These new requirements present low-Reynolds number challenges as well as the need for high-performance high-lift design concepts. Here we report on an effort to expand the relatively well established design space for low-pressure turbine airfoils. Analytical and experimental mid-span performance data and loadings are presented for four new airfoil designs based on the Pack B velocity triangles. The new designs represent a systematic expansion of low-pressure turbine airfoil design space through the application of high-lift design concepts for front- and aft-loaded airfoils. All four designs performed as predicted across a wide range of Reynolds numbers. Full-span loss data for the new high-lift designs reveal increased endwall losses, which, with the application of non-axisymmetric endwall contouring, have been substantially reduced. Taken holistically, the results presented here demonstrate accurate transition modeling provides a reliable method to develop optimized, very high-lift airfoil designs.

INTRODUCTION

Low-Pressure Turbines (LPTs) can contribute as much as 30 percent of the weight of an aeroengine [1] and contain as many as 1900 individual airfoils (Figure 1). When one considers the cost of each LPT airfoil, which is typically a precision investment casting, it is clear that reduced-count technology for LPTs can provide considerable cost and weight savings to both the manufacturer and customer. The "historical" characteristic plotted in Figure 1 reflects airfoil counts of well established, in-service LPTs while the "Current" trend is more indicative of modern engines such as the GP7000 shown. One goal of the current work is to investigate closing the gap that exists between current LPT designs and the count levels afforded by "Geared" designs that employ a reduction gear between the LPT and fan to allow the LPT to operate at a more optimal rotational speed.

One of the key challenges in producing high-performance LPTs is the low Reynolds numbers associated with flight at cruise conditions. Low-pressure turbine Reynolds numbers are often low enough to result in significant regions of laminar flow on the suction side of the airfoils, which in turn makes them susceptible to laminar separation and even full stall [2]. Additionally, with the emergence of unmanned air vehicles, which may operate at altitudes significantly higher than commercial airliners, the Reynolds-number-related design challenges are becoming even more difficult.

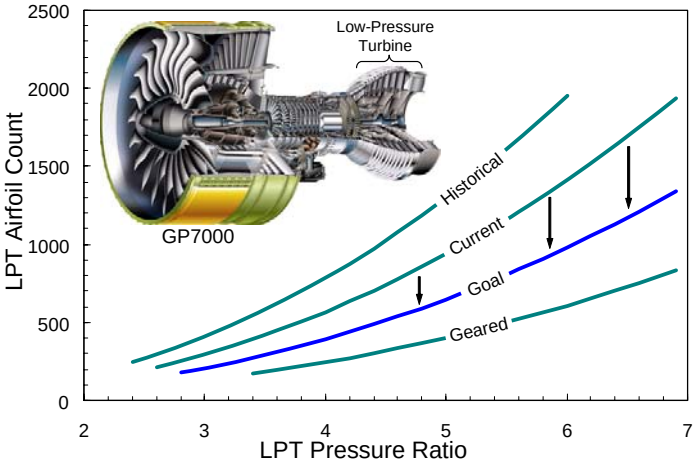

Figure 1. Low-pressure turbine airfoil counts as a function of pressure ratio demonstrating the trend toward reduced count.

Significant headway has been made during the past decade towards the reduction of LPT airfoil counts through high-lift airfoil designs. Initial research on the aerodynamics of more highly loaded LPTs appears to have been based on the family of T104-T106 airfoils developed by Hoheisel et al. [3]. This family includes airfoils with both front and aft loading having values of the non-dimensional Zweifel coefficient, *Zw*, of about 1.04 to 1.07. These and related airfoils have been used in notable investigations by the research groups of both Hodson [1], [4]-[11] and Fottner [12]-[15]. The related airfoils were designed with modified and increasing loadings, with the most

recent designs being described as ultra-highly loaded and reported by Zhang et al. [10] to have Zw = 1.22. Recently, Bons et al. [16] tested an airfoil with Zw=1.35. This airfoil was designed with integrated flow control in anticipation that such a high lift design would need some form of separation control. However, the airfoil proved to perform well without the activation of the flow control.

Many of the initial studies were focused on the influence of Reynolds number on the loss behavior as well as the losses for both steady flow conditions and with the presence of impinging wakes. The secondary-flow behavior has also received some attention (eg. [13]). Also, more recently, the use of passive flow control in the form of surface trips, together with wake unsteadiness, have been investigated with the aim of reducing or eliminating the separation bubble [8]-[11]. The most highly loaded LP airfoil reported in the open literature appears to be that designed and investigated by Houtermans et al. [17] at VKI. This blade row had a Zweifel coefficient of 1.47 and was fron-loaded design.

More engine-specific, high-lift work was presented by Haselbach et al. [18] regarding the application of high lift to the BR715 LPT. The authors reported an increase in the measured performance differential between take-off and cruise conditions which was attributed to increased endwall losses. In their report, Haselbach et al. suggested that non-axisymmetric endwall contouring might be applied to mitigate the elevated endwall losses engendered by their high-lift blading. In a similar work, Gier and Ardey [19] reported on the use of CFD-based transition modeling to design high-lift airfoils for a three-stage LPT rig. The authors applied aft loading to their high-lift designs and found that measured performance was lost more rapidly with decreasing Reynolds number compared to the conventional-lift design. This degradation in performance was attributed to boundary layer separations on the airfoil surfaces.

The baseline airfoil for the present investigation is the Pack B profile, developed to study the aerodynamics of LPT airfoils in low-speed cascade experiments. As with the other airfoils mentioned, Pack B has a separation bubble on the suction surface under most steady-flow operating conditions. Both the steady and unsteady flow behavior of this blade row have been investigated by several research groups (eg. [18]-[22], [24][25]). The application of flow control to this airfoil has also been investigated. The flow control has taken the form of boundary layer tripping devices [26][27], steady blowing through a slot [28][29] and the use of vortex-generator jets [30]-[32].

To investigate the effects of high levels (relative to what is available in literature) loading on aerodynamic performance, as well as provide further validation of the transition modeling of [33] and [34], a suite of new airfoils has been designed for the same service as Pack B but with lift increases ranging from 25 to 61 percent. In this report, the term "high lift" is used to describe designs with loading levels above the baseline Pack B airfoil. The following sections present information regarding the process employed to design the new airfoils as well salient test results for each geometry.

NOMENCLATURE

Latin:

C	Chord
C_P	Static-pressure coefficient: $(P_{01}-P_s)/(P_{01}-P_{s2})$
C_{P0m}	Mixed-out total -pressure loss: $(P_{01}-P_{02m})/(P_{02m}-P_{s2})$
H	Airfoil span
Tu	Turbulence intensity
k	Turbulence kinetic energy
s	Arc distance along airfoil surface
u	Axial velocity
v	Tangential velocity
x	Axial direction
z	Span-wise direction
Zw	Zweifel load coefficient

Greek:

β	Flow angle relative to the axial direction
Λ	Turbulence integral length scale
τ	Airfoil pitch dimension

Superscripts/Subscripts:

$+$	Wall units
1	Cascade inlet location
2	Cascade exit location
0	Total conditions
s	Static conditions
up	In the upstream direction

AIRFOIL DESIGN PROCEDURE

The CFD solver employed for the airfoil design work was the 3-D structured RANS code described by Ni [35] and Ni and Bogoian [36]. This solver is a density-based, finite-volume based code that is second-order accurate. Additionally, multi-grid techniques and preconditioning were employed to accelerate convergence. Numerical closure for turbulence was obtained via the k-ω model. Two-dimensional simulations were employed for the optimization work with an O-H grid topology comprising approximately 18,000 grid points per span-wise plane, per passage. These grid counts provided essentially grid-independent solutions with values of y^+ of the order 1 and approximately 7 grid points per momentum thickness.

The transition modeling capability described by Praisner and Clark [33] and Praisner et al. [34] was employed in the design of the four new high-lift airfoils reported on here. Praisner and Clark [33] provided evidence that the accuracy of empiricism used for the prediction of transition can be enhanced by capturing the effects of free-stream turbulence on pre-transitional boundary layers. Subsequently, for the design work performed for the current study, inlet free-stream turbulence quantities of k and ω were set based on measured values of turbulence intensity (Tu) and integral length scale (ω). Praisner and Clark [33] also reported on a modeling system for quasi-laminar boundary layers which they employed to supplement 104 cascade data sets to build databases for attached- and separated-flow transition. Two correlations were developed from this data base, one for the onset of attached-flow transition and the other separated-flow transition. These models were based on *local* flow-field parameters and were validated with a range of turbomachinery-specific validation cases in [37].

For the design of each new airfoil shown in Figure 2, the general airfoil shape and loading characteristics were set by an experienced designer. Guidance for the airfoil loading characteristics and boundary layer state (separated or attached flow) was provided by both inviscid and transitional-viscous simulations. Once a non-stalled flow condition was achieved,

as predicted by the aforementioned modeling capability, and the desired loading characteristics were achieved, computer-aided optimizations were performed with two-dimensional transitional CFD simulations. The objective of each optimization was the minimization of predicted profile loss at a design Reynolds number (Re_{C2}) of approximately 135,000 based on exit conditions (subscript 2) and airfoil chord (C). All design work was conducted with an inlet free-stream turbulence intensity of approximately 4.0%. This value is typical of free-stream levels present in LPTs [33] and is consistent with the companion experimental testing. Also, careful attention was paid to ensure that each of the four new high-lift designs (Zw > 1.2) were free of pressure-side separations at design conditions.

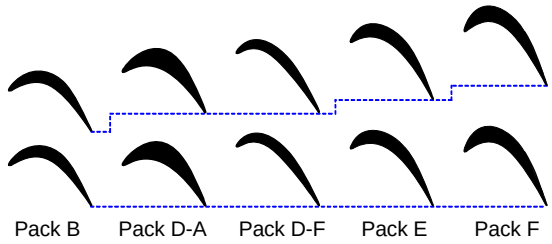

Figure 2. Four new airfoil designs compared to the baseline Pack B design.

Figure 2 shows the general shapes of the five airfoil designs considered in the current study. The Pack B airfoil is a low-speed design characteristic of in-service P&W LPTs of the time and was originally released to research institutions in the mid 1990s for the study of low-Reynolds number LPT boundary layer behavior. While the exit metal angle of the Pack B design is 60 degrees relative to the axial direction, the typical measured and predicted (with transition modeling) exit flow angle is approximately 58.5 degrees. Employing the measured exit flow angle, a Zweifel load coefficient (Zw) of 1.13 is calculated for Pack B using the following equation:

$$Zw = 2\frac{\tau}{C_x}\sin^2\beta_2\left(\frac{u_1}{u_2}\cot\beta_1 + \cot\beta_2\right) \qquad (1)$$

where τ is the airfoil pitch, C_x is the axial chord, β_1 and β_2 are the inlet and exit flow angles, and U_{x1} and U_{x2} are the inlet and exit axial velocities, respectively. The Pack D, E, and F airfoils were designed with 25%, 43%, and 61% lift increases respectively compared to Pack B.

Table 1. Design parameters for each of the five airfoils considered for this study.

	Pack B	Pack D-A	Pack D-F	Pack E	Pack F
Zw	Base	+25%	+25%	+43%	+61%
C/C_x	1.11	1.11	1.22	1.20	1.19
τ/C_x	0.8856	1.106	1.106	1.264	1.424
Suction-s/C_x	1.45	1.53	1.53	1.61	1.71

High-level design parameters for the airfoils are given in Table 1. The Pack D designs have been the focus of testing for a number of years now, and detailed profile and secondary loss data are presented by Popovic et al. [38] and Zoric et al. [39][40]. The Pack D-A design is an aft-loaded design with a stagger angle that matches that of Pack B with a higher thickness-to-chord ratio. Pack D-F is a front-loaded design with a higher stagger angle than Pack B and a similar thickness-to-chord ratio. From Figure 2, Pack E can bee seen to be a high-camber design with high suction-side curvature in the fore region and a stagger angle close to the Pack D-F design and a similar thickness-to-chord ratio of Pack B. Finally the Pack F design presents a similar, albeit thicker, geometry to Pack E.

EXPERIMENTAL DETAILS

The data presented in this report were obtained from two low-speed cascade facilities, one at Carleton University, and a second at Wright Patterson Air Force Base. A brief description of each facility follows.

The Carleton University (CU) facility is an open-loop facility that accommodates 9 Pack B airfoils with an axial chord of 7.5cm and a span of 20.0cm for an aspect ratio of 2.41. Free-stream turbulence can be elevated to 4.0% through the use of two turbulence-generating grids. While both grids provide 4.0% turbulence at the inlet to the cascade, the grids were designed and located so as to provide two levels of turbulence length scale at the same intensity. The first grid (Grid 1) was mounted far upstream of the cascade (x_{up}=18.4C_x) and provided a length-scale-to-chord ratio (Λ_x/C_x) of 0.4 while the second grid (Grid 2) was mounted closer to the test section inlet (x_{up}=4.6C_x) to achieve a length-scale-to-chord ratio of 0.1. Mid-span profile losses were measured 0.4C_x downstream of the cascade using a three-hole pressure probe with a tip width of 2.0mm. The uncertainties for the pressure probe measurements are estimated to be ±0.6° for flow angles and ±0.5% of the local dynamic pressure for the dynamic and total pressures. The resulting uncertainty in the total pressure loss coefficient is approximately ±17% at Re_{C2}=88,000. More details concerning the Carleton University test hardware and data reduction can be found in [23] and [38].

The open-loop, induction wind tunnel which houses the cascade at Wright Patterson Air Force Base (WP) draws air through the bell-mouth inlet equipped with flow straighteners and into the 0.85m tall x 1.22m wide test section at up to 80 m/s. The baseline Pack B linear cascade consists of sixteen 0.88m span by 8.9cm axial chord (C_x) blades. Uniformity of the inlet velocity across the baseline 16 blade cascade is within ±2% at a Reynolds number of 50,000 with less than 1% free-stream turbulence. A turbulence grid mounted at x_{up}=18.4C_x provide a turbulence level of approximately 3.3% and Λ_x/C_x=0.4. A Kiel probe was employed to measure the total pressure 0.7C_x downstream of the cascade trailing edge while an x-hot-wire was used to obtain corresponding velocity and flow angle measurements. Uncertainties in the individual measurements translated to an uncertainty of approximately ±10% for the total pressure loss coefficient at Re_{C2}=88,000. A more detailed description of this cascade facility can be found in Bons et al. [30].

Since the losses for the two cascade facilities were measured at different axial stations, loss values presented in this report were mixed-out according to the process for incompressible flow provided in [41].

TEST RESULTS

Figure 3 shows the surface static-pressure distribution for the pack B design at design Re as predicted by a fully turbulent CFD simulation. The ordinate scale for this plot was set to match those of Figures 5 and 7 to facilitate comparisons between these figures. It should be noted that, while not

present in Figure 3 due to the fully-turbulent assumption, the Pack B design possess a small separation bubble on the pressure side of the airfoil at the design Reynolds number. Pack B presents a distinctly aft-loaded pressure distribution with a peak velocity occurring at approximately 52% of the suction-side surface distance. The peak velocity is followed by a region of relatively strong adverse pressure gradient which gradually relaxes as the trailing edge is approached.

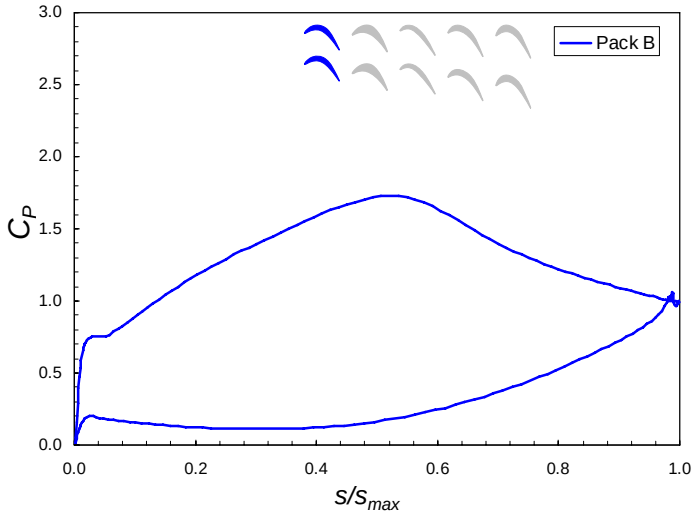

Figure 3. Baseline Pack B airfoil predicted loading distribution.

Figure 4 shows measured mid-span losses for the Pack B airfoil from both the CU and WP facilities. Grid 2 with *Tu*=4.0% was employed for the CU data while the WP data was taken with *Tu*=3.3%. At the approximate design Reynolds number of 140,000, the measured losses from these two facilities are in reasonable agreement. As un-stalled profile losses have been shown to be sensitive to turbulence intensity [38], the higher WP losses compared to those from the CU facility are attributed to the lower *Tu* level employed for testing. The data from the CU facility shows the typical trend of loss-versus Reynolds number with open separations occurring only below Re_{C2}=80,000. The data from WP show stall below a similar critical level of approximately 90,000.

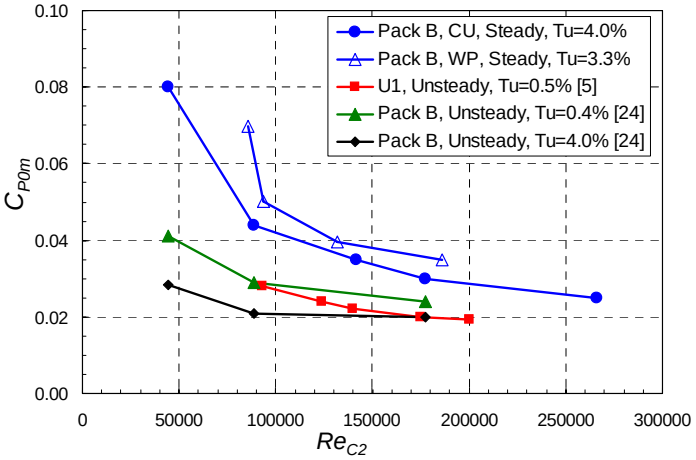

Figure 4. Pack B loss data from both the CU and WP test facilities. Also plotted are unsteady wake-passing loss data for Pack B from Mahallati [24] and the "U1" airfoil design from Howell et al. [5].

Also plotted in Figure 4 are loss data from [5] for the "ultra-high lift" U1 airfoil and for Pack B [24] with the presence of unsteady bar-generated wakes. The losses for the U1 design with *Tu*=0.5% with unsteadiness are, on average, lower than the unsteady Pack B data with *Tu*=0.4%. The unsteady Pack B data with *Tu*=4.0% display the lowest losses plotted in Figure 4.

As in the results presented by [4] and [5] for a similar *Zw* level, the Pack B design realize a notable loss reduction with the introduction of the unsteady wakes. More details concerning the unsteady Pack B data will be presented later in this section. These comparisons demonstrate that, although released in the mid 1990s, the Pack B design is a high performance design considered appropriate here for use as a baseline reference for high-lift studies.

Surface static pressure distributions for the Pack D-A and D-F designs are shown in Figure 5. Here the Pack B loading is also included for reference. Again, both Pack D designs provide 25% increased loading compared to Pack B. The loading shapes for each Pack D airfoil were intentionally set to be distinctly front and aft loaded. The diffusion level on the aft portion of the suction side of Pack D-A is significantly higher than for Pack B and D-F. In contrast, the Pack D-F design is an extremely front loaded design that generates a pronounced over-speed at the leading edge. While the peak velocity level of the D-F design is slightly higher than Pack B, the gross diffusion level on the suction side is similar to the Pack B design due to the front-loaded nature of the design.

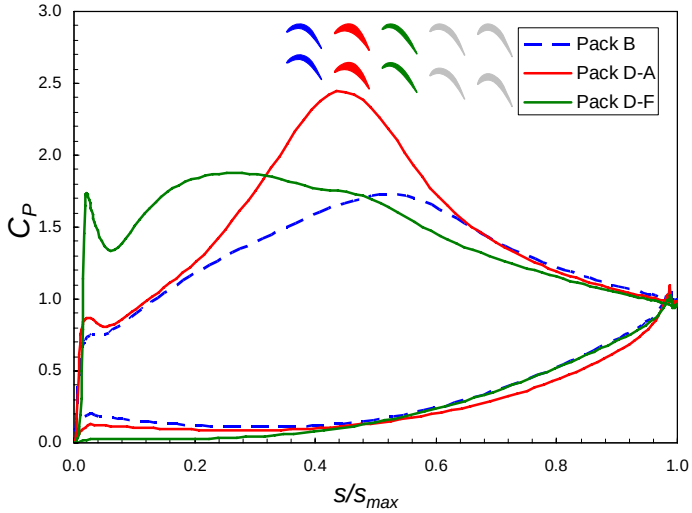

Figure 5. Pack D surface static pressure distributions with the Pack B loading included for reference.

Measured losses from the CU test facility are shown in Figure 6 with the Pack B data from Figure 4. Again, here Grid 2 was employed for the testing. Pack D-A experiences reattaching separations above Re_{C2}=60,000 while experiencing pronounced stall for lower Reynolds numbers. This abrupt stall behavior is similar to the results presented in [38] for *Tu*=1.5% In contrast, the Pack D-F design does not experience stall for *any* of the Reynolds numbers tested. In fact, measured surface static pressures indicated that separations do not exit at the higher Reynolds numbers for the Pack D-F design [38]. So although the D-A design is not stalled at the design Reynolds number, the high level of diffusion on the suction side generates loss levels approximately 15% higher than the D-F design. Although the mid-span losses of Pack D-F are

comparable to those of Pack B, the endwall losses have been shown to be substantially higher than both the Pack B and D-A designs [39]. This is consistent with the work of Weiss and Fottner [13] with front- and aft-loaded airfoils.

Off-design performance characteristics for Packs B, D-A, and D-F are presented by Zoric et al. [40]. Their results indicate that, due to a high aft-region diffusion level, the Pack D-A design is more sensitive to off-design conditions than Pack D-F. Finally, the performance of the Pack D airfoils were well predicted by the transition modeling system employed to design them [34][42].

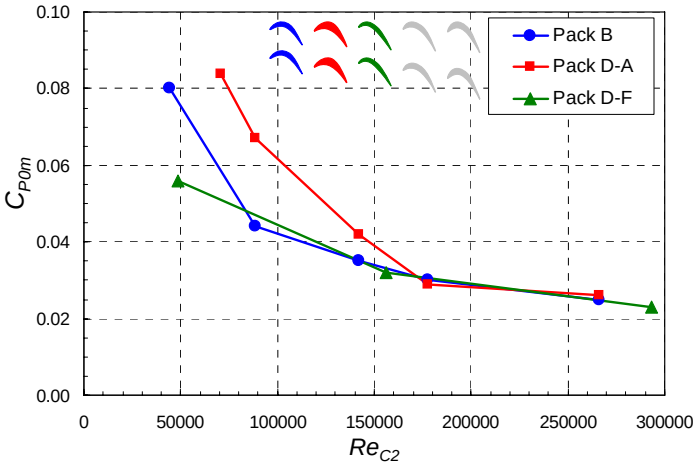

Figure 6. Comparisons of Pack D-A and D-F measured loss data with Pack B.

Based on the experience gained with the Pack D airfoil testing, two new airfoils, Pack E and F, were design with loading increases of 43% and 61% relative to Pack B. The loading distributions for these two designs are shown in Figure 7 along with Pack B. Both new designs were set to be distinctly front-loaded with the aft-region diffusion for Pack E being similar to Pack B. The Pack F design displays a higher peak velocity than the E design and higher aft-region diffusion levels. Assuming a typical exit Mach number for a large commercial LPT of 0.65, the peak C_P value on the suction side of Pack F represents a surface Mach number of approximately 1.1. Based on numerical studies as well as cascade testing, this level of surface Mach number is deemed admissible with regard to shock formation.

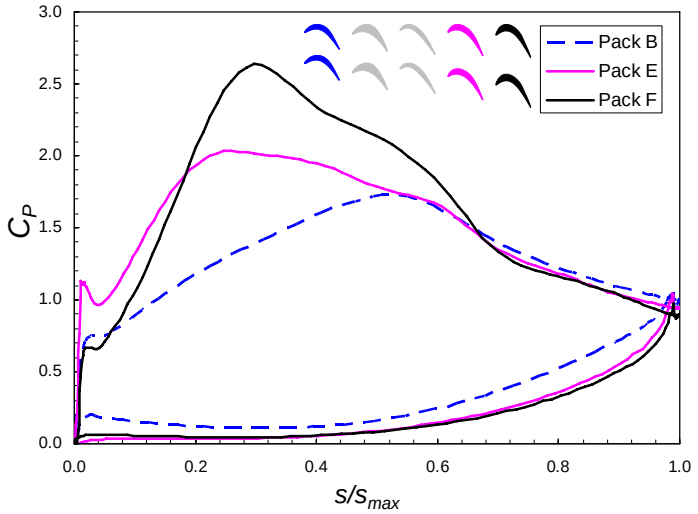

Figure 7. Pack E and F surface pressure distributions with the baseline Pack B shown for reference.

The measured losses versus Reynolds number for the Pack E and F designs are shown in Figure 8. The Pack E design was tested in the WP facility with Tu=3.3% while the Pack F design was tested in the CU facility with Grid 1 (Tu=4.0%). The Pack E losses shown here demonstrate performance on par with the Pack B design, even down to the lowest Reynolds numbers considered. Similarly, the Pack F design provides comparable mid-span performance to the Pack B design. Additionally, the stall-free characteristics of the E and F designs were predicted by the transition modeling capability employed to design them. Taking into consideration the level of high-lift associated with these front-loaded designs, one might expect the endwall losses to be increased for both airfoils relative to Pack B and even D-F.

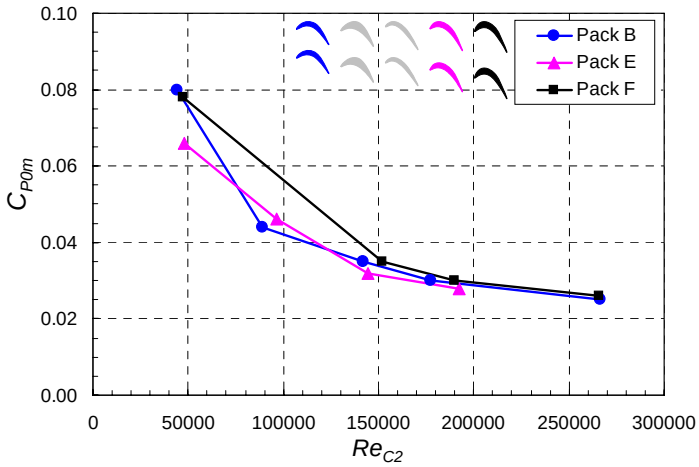

Figure 8. Pack E and F measured loss data versus Reynolds number with Pack B data plotted for reference.

Figure 9 shows a plot of the loss-versus-Reynolds number characteristics for all five airfoils considered in this work. Companion power-law fits are included for each data set in order to enable visual interpolation. At the design Reynolds number (Re_{C2}=135,000) the high-lift designs, save Pack D-A, generate mid-span losses in line with the baseline Pack B design. This is somewhat surprising considering the lift levels achieved by the new designs and the fact that unsteady wakes were not present in this testing. So, it appears that, with engine-specific levels of Tu and no deterministic unsteadiness such as wake passing, front loading enables high-lift designs with good *mid-span* performance. However, the high-lift front-loaded designs have been shown to engender higher endwall losses than conventional-lift, aft-loaded designs [39][40].

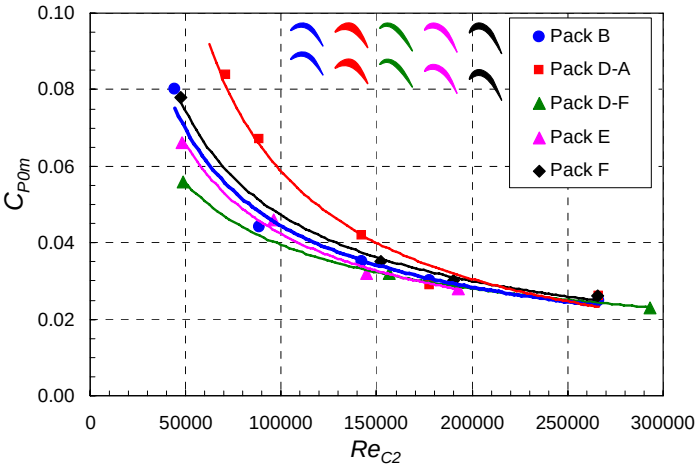

Figure 9. Comparison of loss-versus-Reynolds number characteristics for the four high-lift and baseline Pack B designs with power-law fits for each data set.

To address the increased endwall losses generated by high-lift, front-loaded airfoil designs, non-axisymmetric endwall contouring was applied to the Pack D-F design. Pack D-F was chosen because it showed the most promise considering its low profile losses (Figure 9). More details regarding this effort are reported by Praisner et al. [42]. The contoured endwalls installed in the CU test facility, are shown in Figure 10. For this testing, only the endwalls at the base of the cascade were contoured and losses were measured across the half span.

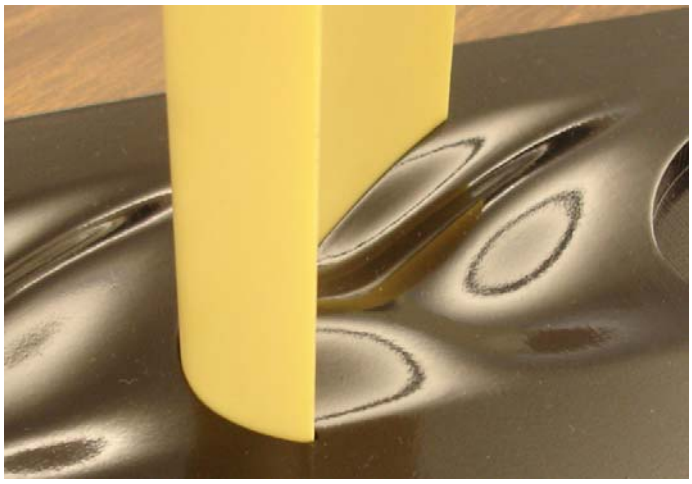

Figure 10. Endwall contouring applied to the Pack D-F design.

Figure 11 shows mixed-out loss-versus-span distributions for Pack B and D-F with planar endwalls as well as Pack D-F with the contoured endwall. These data were taken at a Reynolds number of approximately 180,000 to reduce the impact of any suction-side separations and thus, provide a more isolated assessment of the contouring effects. Additionally, Grid 2 was employed for the contouring study in the CU facility. The results shown in Figure 11 reveal a significant reduction in losses in the endwall region between 0 and 35 percent span. The total mass-averaged integrated loss for the Pack B data in Figure 11 is 0.043 while the planar and contoured values for Pack D-F are 0.063 and 0.049 respectively. So, the mitigation of the endwall losses afforded by the contouring brings the full-span loss of the high-lift Pack D-F design down to a level approximately 14% higher than the baseline Pack B design. When considering the lift increase of 25% provided by this design, this level of loss increase trades favorably with weight and cost reductions.

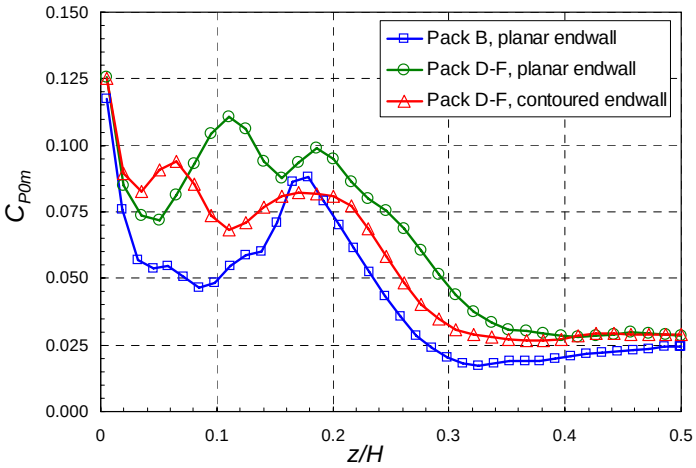

Figure 11. Comparisons of the span-wise loss distributions for Pack B and D-F with planar endwalls and Pack D-F with contoured endwalls.

Finally, experiments were conducted with unsteady bar-generated wakes with the Pack B and D airfoil designs. Loss data versus reduced frequency are plotted in Figure 12 for the three designs. Here reduced frequency is defined as:

$$f_r = \frac{C_x / u_1}{\tau_{bars} / v_{bars}} \qquad (2)$$

Details concerning the choice of this form of reduced frequency are given in [25]. For comparative purposes, the form of reduced frequency employed by researchers such as [4][8] can be approximated from the abscissa in Figure 12 simply by dividing by 3.5.

The data presented in Figure 12 were collected at approximately Re_{C2}=90,000 with Grid 1 in the CU cascade facility. It was necessary to employ Grid 1 for the unsteady-wake testing because the placement of Grid 2 interfered with the rotating bar apparatus. Details of the experimental techniques employed to record these data are presented in Mahallati and Sjolander [24]. With the attendant increase in length scale associated with the use of Grid 1, Pack D-A experiences stall at Re_{C2}=90,000 while it does not stall at this Reynolds number with Grid 2. This is evidenced in the extremely high loss for Pack D-A at zero reduced frequency in Figure12. However, with the introduction of unsteady wakes at even low reduced frequencies, stall is mitigated for the Pack D-A design. While the unsteady wake losses experience continued reduction with increased wake-passing frequencies, they do not reach the levels of Pack B at any of the levels of reduced frequency tested. The results for Pack D-F however, demonstrate similar losses to Pack B for all reduced frequencies considered. To date, unsteady-wake testing has not been performed with the Pack E and F designs. More details concerning the unsteady bar-generated wake studies with the Pack B and D designs are given by [25] and [41].

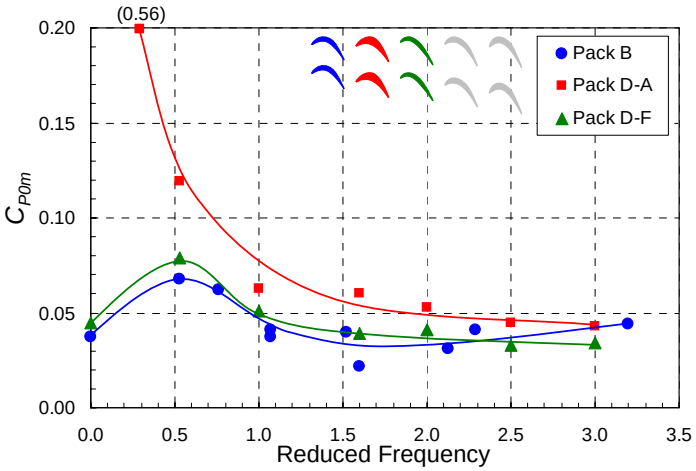

Figure 12. Mid-span losses for Pack B and D designs as a function of the reduced frequency of unsteady bar-generated wake passing.

CONCLUSIONS

Results from a study of the application of high-lift design concepts to LPT airfoils have been presented. Experimental data presented for the baseline Pack B airfoil have demonstrated it to be a low-loss design. Furthermore, the unsteady losses of the Pack B design have been shown to be similar in level to published results from other LPT-related high-lift studies. The new high-lift airfoils employed for this study were developed using both designer input as well as computer aided optimization techniques coupled with a CFD-based transition modeling system. Four new airfoils were designed with up to a 61% lift increase relative to the Pack B design. Mid-span loss data for the new high-lift airfoils, indicate that designs are possible with relatively low profile loss. Also, these low profile losses are achievable simply with engine-specific levels of free-stream turbulence intensities, and without capitalizing on the benefits of unsteady wake impingement from upstream rows. From a mid-span performance perspective, the most successful high-lift designs tested are shown to be the front-loaded airfoils. However, with the front loaded designs are shown to have higher endwall losses than similar designs which employ aft-loading conventions. Experimental data are presented which demonstrate the effectiveness of endwall contouring in reducing the high endwall losses of a high-lift front-loaded design. The integrated loss of the contoured high-lift design is shown to be reduced to a level which is reasonably close to the baseline design. Finally, a select front-loaded high-lift design demonstrates essentially the same mid-span performance as the baseline Pack B airfoil when exposed to unsteady wake-passing flow conditions. Finally, future considerations include studying the impacts of high-lift wakes and endwall flows on multi-stage performance.

ACKNOWLEDGMENTS

The authors would like to thank Pratt & Whitney for permission to publish this work. More specifically, the support of Shankar Magge, Dick Price, Joel Wagner, and Rich Gacek, is greatly appreciated.

REFERENCES

[1] Curtis, E.M., Hodson, H.P., Banieghbal, M.R., Denton, J.D., and Howell, R.J., “Development of Blade Profiles for Low Pressure Turbine Applications,” ASME J. Turbomachinery, Vol. 119, July 1997, pp. 531-538.

[2] Hourmouziadis, J., “Aerodynamic Design of Low Pressure Turbines,” AGARD-LS-167, "Blading Design for Axial Turbomachines," June 1989, Paper 8.

[3] Hoheisel, H., Kiock, R., Lichtfuss, H.J. and Fottner, L., “Influence of Free-Stream Turbulence and Blade Pressure Gradient on Boundary Layer and Loss Behaviour of Turbine Cascades,” ASME J. Turbomachinery, Vol. 109, April 1987, pp. 210-219.

[4] Schulte, V., and Hodson, H.P., “Unsteady Wake-Induced Boundary Layer Transition in High Lift LP Turbines,” ASME Paper No. 96-GT-486.

[5] Howell, R.J., Hodson, H.P., Schulte, V., Schiffer, H.-P., Haselbach, F, and Harvey, N.W., “Boundary layer Development in the BR710 and BR715 LP Turbines - The Implementation of High Lift and Ultra High Lift Concepts,” ASME Paper 2001-GT-0441, June 2001.

[6] Howell, R.J., Ramesh, O.N., Hodson, H.P., Harvey, N.W. and Schulte, V., “High Lift and Aft Loaded Profiles for Low Pressure Turbines,” ASME J. Turbomachinery, Vol. 123, No. 1, January 2004, pp. 181-188.

[7] Stieger, R.D. and Hodson, H.P., “The Transition Mechanism of Highly-Loaded LP Turbine Blades,” ASME J. Turbomachinery, Vol. 126, No. 4, October 2004, pp. 536-543.

[8] Zhang, X.-F., and Hodson, H.P., “The Combined Effects of Surface Trips and Unsteady Wakes on Boundary layer Development of an Ultra-High-Lift LP Turbine Blade,” ASME Paper GT2004-53081, 2004.

[9] Vera, M. Hodson, H.P. and Vazquez, R., “The Effects of a Trip Wire and Unsteadiness on a High Speed Highly Loaded Low-Pressure Turbine Blade,” ASME Paper GT2004-53822, 2004.

[10] Zhang, X.-F., Vera, M., Hodson, H.P., and Harvey, N.W., “Separation and Transition Control on an Aft-Loaded Ultra-High_Lift LP Turbine Blade at Low Reynolds Numbers: Low-Speed Investigation,” ASME Paper GT2005-68892, 2005.

[11] Vera, M., Zhang, X.-F., Hodson, H.P., and Harvey, N.W., “Separation and Transition Control on an Aft-Loaded Ultra-High_Lift LP Turbine Blade at Low Reynolds Numbers: High-Speed Validation,” ASME Paper GT2005-68893, 2005.

[12] Ladwig, M., and Fottner, L., “Experimental Investigations of the Influence of Incoming Wakes on the Losses of a Linear Turbine Cascade,” ASME Paper 93-GT-394, 1993.

[13] Weiss, A.P., and Fottner, L., “The Influence of Load Distribution on Secondary Flow in Straight Turbine Cascades,” ASME Trans., J. Turbomachinery, Vol. 117, January 1995, pp. 133-141.

[14] Brunner, S., Fottner, L., and Schiffer, H.-P., “Comparison of Two Highly loaded Low Pressure Turbine Cascades Under the Influence of Wake-Induced Transition,” ASME Paper 2000-GT-268, 2000.

[15] Stadtmuller, P., and Fottner, L., “A Test Case for the Numerical Investigation of Wake Passing Effects on a Highly Loaded LP Turbine Cascade Blade,” ASME Paper 2001-GT-0311, 2001.

[16] Bons, J.P., Hansen, L.C., Clark, J.P., Koch, P.J., and Sondergaard, R., 2005, “Designing Low-Pressure Turbine Blades with Integrated Flow Control,” ASME Paper No. GT2005-68962.

[17] Houtermans, R., Coton, T., and Arts, T., “Aerodynamic Performance of a Very High Lift LP Turbine Blade with Emphasis on Separation Prediction,” ASME J. Turbomachinery, Vol. 126, No. 3, July 2004, pp. 406-413.

[18] Haselbach, F., Schiffer, H.P., Horsman, M., Dressen, S., Harvey, N. and Read, S., 2001 “The Application of Ultra-High Lift Blading in the BR715 LP Turbine,” ASME Paper No. 2001-GT-0436.

[19] Gier, J. and Ardey, S, 2001, "On the Impact of Blade Count Reduction on Aerodynamic Performance and Loss Generation in a Three-Stage LP Turbine," ASME Paper No. 2001-GT-0197.
[20] Murawski, C.G., Sondergard, R., Rivir, R.B., Simon, T.W., and Vafai, K., "Experimental Study of the Unsteady Aerodynamics in a Linear Cascade with Low Reynolds Number Low Pressure Turbine Blades," ASME 97-GT-95, 1997.
[21] Lake, J.P., King, P., and Rivir, R.B., "Effects of Turbulence and Solidity on the Boundary Layer Development in a Low-Pressure Turbine," AIAA Paper 99-0242, 1999.
[22] Dorney, D.J., Lake, J.P., King, P.I., and Ashpis, D.E., "Experimental and Numerical Investigations of Losses in Low-Pressure Turbine Blade Rows," AIAA Paper 2000-0737, 2000.
[23] Mahalatti, A., McAuliffe, B.R., Sjolander, S.A., and Praisner, T.J., 2007 "Aerodynamics of a Low-Pressure Turbine Airfoil at Low Reynolds Numbers Part 1: Steady Flow Measurements," ASME Paper No. GT2007-27347.
[24] Mahalatti, A. and Sjolander, S.A. 2007 "Aerodynamics of a Low-Pressure Turbine Airfoil at Low Reynolds Numbers Part 2: Blade-Wake Interaction," ASME Paper No. GT2007-27348.
[25] Popovic, I., "Measured Steady and Unsteady Aerodynamic Performance of a Family of Three Highly-Loaded Low-Pressure Turbine Cascades," M.A.Sc.(Aero.) Thesis, Department of Mechanical and Aerospace Engineering, Carleton University, Ottawa, Canada, July 2005.
[26] Lake, J.P., King, P.I., and Rivir, R.B., "Low Reynolds Number Loss Reduction on Turbine Blades with Dimples and V-Grooves," AIAA Paper 00-0738, Aerospace Sciences Meeting, Jan. 2000.
[27] Volino, R.J., "Passive Flow Control of Low-Pressure Turbine Airfoils," ASME Paper GT-2003-38728, 2003.
[28] McAuliffe, B., "An Experimental Study of Flow Control Using Blowing for a Low-Pressure Turbine Airfoil," M.A.Sc.(Aero.) Thesis, Department of Mechanical and Aerospace Engineering, Carleton University, Ottawa, Canada, 2003.
[29] McAuliffe, B.R., and Sjolander, S.A., "Active Flow Control Using Steady Blowing for a Low-Pressure Turbine Cascade," ASME J. Turbomachinery, Vol. 126, No. 4, October 2004, pp. 560-569.
[30] Bons, J.P., Sondergaard, R., and Rivir, R.B., "Turbine Separation Control Using Pulsed Vortex generator Jets," ASME J. Turbomachinery, Vol. 123, No. 2, April 2001, pp. 198-206.
[31] Sondergaard, R., Bons, J.P., Sucher, M., and Rivir, R.B., "Reducing Low-Pressure Turbine Stage Blade Count Using Vortex Generator Jets," ASME Paper GT2002-30602.
[32] Volino, R.J., "Separation Control on Low-Pressure Turbine Airfoils Using Synthetic Vortex generator Jets," ASME Paper GT2003-38728, 2003.
[33] Praisner, T. J., and Clark, J. P., 2007, "Predicting Transition in Turbomachinery, Part I – A Review and New Model Development," Journal of Turbomachinery, Vol. 129, No. 1, pp. 1-13.
[34] Praisner, T. J., Grover, E. A., Rice, M. J., and Clark, J. P., 2007, "Predicting Transition in Turbomachinery, Part II – Model Validation and Benchmarking," Journal of Turbomachinery, Vol. 129, No. 1, pp. 14-22.
[35] Ni, R. H., 1982, "A Multiple-Grid Scheme for Solving the Euler Equations," AIAA Journal, Vol. 20, No. 11, pp. 1565-1571.
[36] Ni, R. H. and Bogoian, J. C., 1989, "Prediction of 3-D Multistage Turbine Flowfield Using a Multiple-Grid Euler Solver," AIAA Paper No. 89-0203.
[37] Binder, A., Schröder, T. H., and Hourmouziadis, J., 1988, "Turbulence Measurements in a Multistage Low-Pressure Turbine," ASME Paper No. 88-GT-79.
[38] Popovic, I., Zhu, J., Dai, W., Sjolander, S.A., Praisner, T.J. and Grover, E.A., 2006, "Aerodynamics of a Family of Three Highly Loaded Low-Pressure Turbine Airfoils: Measured Effects of Reynolds Number and Turbulence Intensity in Steady Flow," ASME Paper No. GT2006-91271.
[39] Zoric, T., Popovic, I., Sjolander, S.A., Praisner, T.J. and Grover, E.A., 2007, "Comparative Investigation of Three Highly Loaded LP Turbine Airfoils: Part I –Measured Profile and Secondary Losses at Design Incidence," ASME Paper No. GT2007-27537.
[40] Zoric, T., Popovic, I., Sjolander, S.A., Praisner, T.J. and Grover, E.A., 2007, "Comparative Investigation of Three Highly Loaded LP Turbine Airfoils: Part I –Measured Profile and Secondary Losses at Off-Design Incidence," ASME Paper No. GT2007-27538.
[41] Mahallati, A., 2003, "Aerodynamics of a Low-Pressure Turbine Airfoil Under Steady and Unsteady Main Flow Conditions," Ph.D. Thesis, Carleton University, Ottawa, Canada.
[42] Praisner, T.J., Allen-Bradley, E., Grover, E.A., Knezevici, D.C., and Sjolander, S.A., 2007, "Application of Non-Axisymmetric Endwall Contouring to Conventional and High-Lift Turbine Airfoils," ASME Paper No. GT2007-27579.